

Does sand promote or hinder the mobility of cohesive sediment gravity flows?

MEGAN L. BAKER*  and JACO H. BAAS† 

*Department of Geography, Durham University, South Road, Durham, DH1 3LE, UK

(E-mail: megan.l.baker@durham.ac.uk)

†School of Ocean Sciences, Bangor University, Menai Bridge, Isle of Anglesey, LL59 5AB, UK

Associate Editor – Kyle Straub

ABSTRACT

Sediment gravity flows exhibit a large range of flow behaviours, making their flow dynamics hard to predict and the resulting deposits a challenge to interpret. Cohesive sediment gravity flows containing clay are particularly complex, as their behaviour is controlled by the balance of turbulent and cohesive forces. A first set of laboratory lock-exchange experiments investigated the effect of adding 25% very fine sand by volume to high-density cohesive sediment gravity flows with strongly suppressed turbulence. This caused these mixed clay–sand flows to become more cohesive, have shorter runout distances, and have lower head velocities than the original pure-clay flows, despite the increase in density difference and the non-cohesive properties of the sand. Yield stress measurements confirmed that adding the non-cohesive very fine sand increases the cohesive strength of dense clay suspensions. This higher cohesive strength outcompetes the enhanced density difference and reduces the flow mobility. A second set of experiments across a larger range of clay concentrations showed that, for low-density cohesive sediment gravity flows dominated by turbulent mixing, the addition of 25% very fine sand increased the head velocities because of the enhanced density difference and weak cohesive forces. Thus, the addition of very fine sand may increase or decrease the mobility of cohesive sediment gravity flows, depending on the initial type of flow and the balance between turbulent and cohesive forces. In the natural environment, this study proposes that very fine sand can only increase the cohesive strength and reduce the flow mobility of cohesive sediment gravity flows that have a sufficiently strong matrix strength to fully support the sand particles. The contribution of very fine sand to the cohesive strength of high-density cohesive sediment gravity flows may have important implications for flow transformation on submarine fans, especially in distal regions where transient–turbulent, cohesive flows are particularly common.

Keywords Clay, cohesive forces, flow mobility, laboratory experiments, sand, sediment gravity flow, yield stress.

INTRODUCTION

Sediment gravity flows (SGFs) are flows driven by gravity acting on the density contrast between a sediment-laden fluid and the ambient fluid. SGFs are volumetrically the most important sediment

transport process on our planet and dominate sediment supply to many parts of the deep ocean (Talling, 2014). In the natural environment, SGFs vary greatly in rheology and mobility, governed by, for example, flow velocity, sediment concentration, particle support mechanism and cohesive

clay content (Mulder & Alexander, 2001; Talling, 2013). There is thus a continuum of SGF behaviour extending from turbidity currents to debris flows, with turbulence-modulated transitional flows bridging the gap (e.g. Baker & Baas, 2020). Turbidity currents, defined as flows in which the particles are supported by the upward component of fluid turbulence generated mainly at the boundaries of the flows (Middleton & Hampton, 1973), have been rigorously studied (e.g. Middleton, 1966; Parker *et al.*, 1986; Kneller & Buckee, 2000; Wells & Dorrell, 2021). These turbulent flow conditions are present throughout the flow, including near the bed, producing well-mixed flows without an internal density interface (Talling *et al.*, 2012). Debris flows, which have not been as well studied as turbidity currents, are defined as high-concentration, laminar SGFs with weak to no internal turbulence, where a high concentration of cohesive clay can provide grain support by yield strength (Middleton & Hampton, 1973; Marr *et al.*, 2001; Mulder & Alexander, 2001). Transitional flows, defined as flows with transient turbulent behaviour, fall between turbidity currents and debris flows (Wang & Plate, 1996; Lowe & Guy, 2000; Marr *et al.*, 2001; Mohrig & Marr, 2003; Baas *et al.*, 2009, 2011; Sumner *et al.*, 2009; Kane & Pontén, 2012; Kane *et al.*, 2017). The presence of clay in these flows can increase the flow viscosity and yield stress, and thus modulate the turbulent forces driving the flows (Baas & Best, 2002).

Transitional flows have received increasing attention since laboratory experiments demonstrated that only a small amount of cohesive clay is needed to produce transitional flow behaviour (Wang & Plate, 1996; Baas *et al.*, 2009, 2011; Sumner *et al.*, 2009). These flows are therefore likely to be common in the natural environment. This has been evidenced by the growing body of literature describing the deposits of transitional flows, termed hybrid event beds or transitional flow deposits, in the deep-marine environment (e.g. Lowe & Guy, 2000; Barker *et al.*, 2008; Haughton *et al.*, 2009; Kane & Pontén, 2012). Transitional flow deposits across the distal fringe of deep-marine systems often show a downstream transition in deposit properties that reflect flow transformation to more cohesive flow behaviour (e.g. Kane *et al.*, 2017; Baker & Baas, 2020). Understanding the processes responsible for flow transformation from turbulent to transitional or laminar flow is vital for predicting how changes in kinematic behaviour affect the mobility of SGFs

travelling through a system, and correctly interpreting transitional flow deposits.

The dynamic balance between turbulent forces and cohesive forces within a flow controls transitional flow behaviour. Turbulent forces are produced mainly at the boundaries of the flow and these are driven by the density difference, whilst the strength and number of cohesive bonds in the flow control the cohesive forces (Baas *et al.*, 2009, 2011; Sumner *et al.*, 2009; Baker *et al.*, 2017; Craig *et al.*, 2020). The shifting balance between turbulent and cohesive forces can promote flow transformation between different transitional flow behaviours or cause more dramatic flow transformation to the end member flow types of turbidity current or debris flow. Flow classification schemes of clay-laden flows (e.g. Baas *et al.*, 2009; Hermidas *et al.*, 2018) categorize this continuum of flow behaviour.

Laboratory experiments have shown that the sediment composition within a flow can control the balance of turbulent and cohesive forces. Increasing the clay concentration within a SGF can promote flow transformation from non-cohesive turbidity current to highly cohesive debris flow and reduce the flow mobility, provided the clay bonds suppress the turbulent forces (Baas *et al.*, 2009; Sumner *et al.*, 2009; Baker *et al.*, 2017; Hermidas *et al.*, 2018). Other laboratory experiments have used a fixed volume concentration and changed the ratio of sand to clay within the flows. These experiments demonstrated that increasing the non-cohesive sand content in mixed clay-sand flows at the expense of clay, produces increasingly turbulent flows with higher mobility (Marr *et al.*, 2001; Ilstad *et al.*, 2004). This increase in flow mobility was attributed to a reduced cohesive strength of the starting suspensions, which enables the density-driven shear forces to break the clay flocs and produce turbulence-supported flows (Marr *et al.*, 2001). Many experiments, including those cited above, have demonstrated that the rheology of cohesive SGF suspensions correlates with the flow behaviour of the suspensions. Parameters such as yield stress of the starting suspension have been shown to predict the flow behaviour and runout distance (Baker *et al.*, 2017).

Experiments examining how the ratio of sand to clay controls the flow behaviour of cohesive SGFs often use a fixed volume concentration, so that the driving force – determined by the density difference – is a controlled variable (e.g. Ilstad *et al.*, 2004). In the natural environment, a

changing SGF concentration, and hence driving force, is likely to be a common occurrence as flows incorporate water or dewater, as well as deposit sediment or erode the substrate. When sand is added to a SGF, via erosion of the bed below, the density difference between the flow and the ambient water increases, encouraging the flows to accelerate. In cohesive SGFs, this should increase the shear-induced turbulence, break the clay bonds and increase the flow mobility, provided the sediment can be kept in suspension (Middleton, 1966). It is currently unknown how the addition of sand, and hence the increase in density difference, changes the behaviour of cohesive transitional flows that already have strongly suppressed turbulence because of a high clay concentration. Within these flows, the clay gel can limit the development of turbulence, and this may influence how the balance of turbulent and cohesive force changes.

This paper investigates how the addition of a small amount of very fine sand changes the flow behaviour and mobility of low-density through to high-density cohesive SGFs in the laboratory, to help better understand their flow dynamics and deposits in the natural environment. The experiments contrasted the flow behaviour of pure-clay flows with clay flows to which the sand had been added. The principal aims of this research are:

- 1 To determine how increasing the volume concentration from the addition of very fine sand changes the flow behaviour, flow velocity, runout distance and deposit geometry of high-density cohesive SGFs.

- 2 To determine how increasing the volume concentration from the addition of very fine sand changes the flow velocity of cohesive SGFs across a larger range of sediment concentrations and flow behaviours.

- 3 To investigate how the addition of very fine sand changes the yield stress of the high-density clay-laden starting suspensions, and to discuss possible explanations for the observed changes.

- 4 To discuss the wider potential implications of these results for natural SGFs and their deposits.

MATERIALS AND METHODS

Lock-exchange flume experiments

In order to determine the effect of very fine sand on cohesive SGF dynamics, sediment gravity

flows were produced in a 5.0 m long, 0.2 m wide and 0.5 m deep, smooth-bottomed lock-exchange tank. The tank comprises a 0.31 m long reservoir that was filled with a suspension up to a depth of 0.35 m. The reservoir is separated by a lock gate from the main compartment of the flume, which was filled with seawater to the same depth. The SGFs were composed of either pure clay and seawater or a mixture of clay, sand and seawater (Tables 1 and 2). The seawater used was filtered from the Menai Strait (north-west Wales, UK). Bentonite clay provided by RS Minerals Limited (Guisborough, UK) was used as clay material. This bentonite is composed of Na-Montmorillonite and it is a strongly cohesive clay with a median particle size, D_{50} , of 5.6 μm . Inert, well-sorted, spherical glass beads from Potters Industries Inc. (Malvern, PA, USA) were used to simulate very fine sand grains. Two sets of experiments were conducted. The first set of experiments focused on high-density cohesive SGFs and used glass beads with a D_{50} of 98 μm . The second set of experiments used a wider range of clay flow densities and comprised glass beads with a D_{50} of 116 μm .

A consistent method was used to prepare each suspension to account for any time-dependent behaviour of the mixtures. This method comprised mixing half of the seawater and sediment in a concrete mixer for 15 min, before adding the second half and mixing for a further 15 min. The mixture was then decanted into a container and mixed with a handheld mixer for a further 10 min. The suspension was gradually added to the reservoir as the rest of the tank was filled with seawater. To start an experiment, the mixture in the reservoir was mixed for a further 60 s using the handheld mixer before lifting the gate.

Once the gate had been lifted, a high-definition video camera tracked the front of the flow along the length of the tank. The velocity of the head of the flow was determined using the time-stamped video frames and scale at the bottom of the flume. The SGF deposit height with distance along the tank was measured along the centre line of the flume using a SeaTek 5 MHz Ultrasonic Ranging System (SeaTek Instrumentation, Gainesville, FL, USA), which calculates the vertical distance to the deposit by means of the two-way travel time of an ultrasound pulse. Flow runout distances, defined as the maximum deposit extent from the lock gate, were recorded for all flows that stopped before reaching the end of the tank.

Table 1. Basic experimental data for the first set of experiments, focussing on high-density cohesive sediment gravity flows (SGFs). TC, turbidity current. * = values not measured as part of the present study, but predicted using eqs 1 and 6 of Baker *et al.* (2017). The sand (%) added results in a 25% increase in the total volume concentration.

Total volume concentration	Clay (%)	Sand (%)	Runout distance (m)	Maximum head velocity (m s ⁻¹)	Yield stress (Pa)	Flow type
14.4% clay	14.4	0.0	4.86*	0.35*	1.8	High-density TC
15% clay	15.0	0.0	4.66	0.35	2.3	High-density TC
18% clay-sand	14.4	3.6	3.52	0.36	5.0	High-density TC
18% clay	18.0	0.0	1.42	0.27	21.3	Mud flow
16% clay	16.0	0.0	3.77	0.37	4.6	High-density TC
20% clay-sand	16.0	4.0	1.79	0.31	11.8	Debris flow
20% clay	20.0	0.0	0.22	0.07	67.5	Slide

To obtain grain-size samples from the mixed clay-sand deposits, each deposit was left to settle for 24 h, the water slowly drained from the tank over another period of 24 h, and the deposit left to partially dry for seven days. Sediment cores were taken every 0.2 m from the lock gate along the centre line of the deposit, using 30 mm diameter 60 ml syringe cores. The cores were frozen, before being subsampled by cutting each core into horizontal slices, 2.5 or 5.0 mm thick, depending on the strength of the core. Grain-size analysis was conducted on the samples using a Malvern 2000 laser particle sizer (Malvern Panalytical Limited, Malvern, UK). The grain-size data were converted into percentage clay and percentage sand using 57 µm as the cut-off between the two sediment types, because the glass beads have a lower grain-size limit of 63 µm.

Experiment Set 1: Lock-exchange flume experiments adding 25% very fine sand or clay to high-density pure-clay flows

For the first set of experiments, very fine sand was added to 14.4% and 16% pure-clay flows to study the effect of very fine sand on high-density cohesive SGF behaviour and deposits. These flows were chosen as they are at the top of the maximum head velocity against flow concentration curve for bentonite clay (Baker *et al.*, 2017, fig. 10A), where the turbulent forces driving the flow and the cohesive forces limiting flow mobility are inferred to be finely balanced. The volume concentration of the *mixed clay-sand flows*, C_{cs} , was determined using the following equation:

$$C_{cs} = C_c + C_s \quad (1)$$

where C_c is the concentration of the original *pure-clay flows* and C_s is the concentration of sand, calculated by:

$$C_s = 0.25 \times C_c \quad (2)$$

In addition, pure-clay flows of the same volume concentration as the mixed clay-sand flows were produced as a control, to establish if there is a difference between increasing the volume concentration by 25% with clay or very fine sand; these flows are termed *control clay flows*. The details of all of the high-concentration cohesive SGF experiments are given in Table 1.

The 15% clay flow of Baker *et al.* (2017), who applied the same experimental set-up as the present study, was used to represent the 14.4% pure-clay flow in this study, under the assumption that the difference in behaviour between 14.4% and 15% clay flows is small and within the error range of the experiments. This assumption was tested using equations relating flow behaviour to bentonite clay concentration by Baker *et al.* (2017). These equations predict the maximum head velocity and runout distance of bentonite clay flows based on dimensional analysis of experimental data for bentonite clay flows from 1 to 20% volume concentration. These predictions show that a 14.4% bentonite clay flow has the same maximum head velocity as the 15% bentonite clay flow and a runout distance within 0.2 m.

Table 2. Basic experimental data for the second set of experiments, adding very fine sand to pure-clay sediment gravity flows (SGFs) across a larger range of flow concentrations than in Experiment Set 1. Missing runout distances denote experiments that reached the end of the tank and therefore had a runout distance of at least 4.6 m. TC, turbidity current. The sand (%) added results in a 25% increase in the total volume concentration.

Total volume concentration	Clay (%)	Sand (%)	Runout distance (m)	Maximum head velocity (m s ⁻¹)	Average head velocity for flow duration (m s ⁻¹)	Flow type
10% clay	10.0	0.0	–	0.30	0.25	Low-density TC
12.5% clay–sand	10.0	2.5	–	0.40	0.31	Low-density TC
12% clay	12.0	0.0	–	0.33	0.28	Low-density TC
15% clay–sand	12.0	3.0	–	0.37	0.33	Low-density TC
13.5% clay	13.5	0.0	–	0.37	0.30	Low-density TC
16.9% clay–sand	13.5	3.4	–	0.40	0.35	Low-density TC
14.4% clay	14.4	0.0	–	0.35	0.30	Low-density TC
18% clay–sand	14.4	3.6	–	0.40	0.34	Low-density TC
16% clay	16.0	0.0	4.36	0.35	0.27	High-density TC
20% clay–sand	16.0	4.0	3.68	0.38	0.29	High-density TC
17% clay	17.0	0.0	3.25	0.30	0.25	High-density TC
21.3% clay–sand	17.0	4.3	2.39	0.34	0.25	Debris flow

Determining the starting suspension yield stress of the high-density cohesive sediment gravity flows

Subaerial dam break experiments following the methods of Balmforth *et al.* (2007) and Matson & Hogg (2007) were conducted to determine the yield stress of the starting suspensions used in the first set of lock-exchange experiments for the high-density cohesive SGFs. This method calculates the yield stress from the runout distance of the suspensions based on the idea that non-Newtonian fluids become stationary when the gravitational forces are in equilibrium with the yield stress. The experimental set-up used a small lock-exchange tank, 0.105 m wide, 0.59 m long and 0.12 m deep, with a reservoir, 0.095 m long. A 0.7-L suspension of pure clay or clay–sand of the same composition as the suspensions used in lock-exchange Experiment Set 1 was prepared in a 1.5-L screw cap bottle and manually shaken for 10 min. The suspension was then put into the reservoir to a height of 0.05 m, the gate lifted, and the runout distance of the suspension, X , measured. The yield stress, τ_y , was then determined using the following equations, theoretically derived from a numerical model by Balmforth *et al.* (2007) and Matson & Hogg (2007):

$$\tau_y = \frac{B\rho gH^2}{L} \quad (3)$$

where ρ is the density of the suspension, g is the acceleration due to gravity, H is the height

of the suspension and L is the reservoir length. The Bingham number, B , is defined as the ratio of yield stress to the stresses generated by the weight of the flowing layer. In these experiments the Bingham number was always less than one-third, as the final profile of the deposit showed evidence that all fluid had flowed (Matson & Hogg, 2007, fig. 2), and B can be calculated from the runout distance of the suspension by:

$$B = \frac{9}{8X^3} \quad (4)$$

Results of the subaerial dam break experiments are given in Table 3.

Experiment Set 2: Lock-exchange flume experiments adding 25% very fine sand to pure-clay flows across a large range of concentrations

A second experiment set was conducted to investigate the effect of adding 25% volume concentration of very fine sand to pure-clay SGFs across a larger range of flow concentrations, and hence flow behaviours. Six pure-clay flows were produced, from 10 to 17% volume concentration, and contrasted with six clay–sand flows where the volume concentration was increased by the addition of 25% sand, producing flows with total volume concentrations of 12.5 to 21.3%. The concentrations used were determined using Eqs 1 and 2, as for Experiment Set 1.

Table 3. Experimental data for the subaerial dam break experiments following the methods of Balmforth *et al.* (2007) and Matson & Hogg (2007). Runout distances of the clay and clay-sand suspensions were converted to yield stress using Eqs 3 and 4.

Total volume concentration	Clay (%)	Sand (%)	Density of suspension (kg m^{-3})	Runout distance (m)	Bingham number	Yield stress (Pa)
14.4% clay	14.4	0.0	1194.4	0.55	0.006	1.8
15% clay	15.0	0.0	1202.5	0.44	0.011	2.3
16% clay	16.0	0.0	1216.0	0.40	0.015	4.6
16% clay-sand	12.8	3.2	1225.6	0.54	0.006	1.9
17% clay	17.0	0.0	1229.5	0.30	0.038	11.7
17% clay-sand	13.6	3.4	1239.7	0.49	0.008	1.7
18% clay	18.0	0.0	1243.0	0.24	0.067	21.3
18% clay-sand	14.4	3.6	1250.2	0.40	0.016	5.0
19% clay	19.0	0.0	1256.5	0.21	0.099	32.1
19% clay-sand	15.2	3.8	1267.9	0.32	0.029	6.1
20% clay	20.0	0.0	1270.0	0.17	0.208	67.5
20% clay-sand	16.0	4.0	1282.0	0.30	0.036	11.8
21% clay	21.0	0.0	1296.1	0.24	0.071	15.1
22% clay	22.0	0.0	1310.2	0.19	0.138	29.8
23% clay	23.0	0.0	1324.3	0.17	0.213	46.1

Details of the experimental results from Experiment Set 2 are given in Table 2. Experiment Set 2 used a different batch of bentonite clay from the same supplier, used glass beads with a slightly larger grain size (D_{50} of 116 μm compared to 98 μm), and was conducted at a different time of year compared to the first set of experiments. The bentonite is composed of *ca* 92% Na-Montmorillonite from multiple deposits worldwide. Different batches have slightly different chemical compositions and mineralogy, which can strongly influence the rheological properties of the experimental suspensions. The disparate clay and seawater properties between these two sets of experiments produced suspensions with slightly different cohesive properties for the same clay concentrations and therefore cannot be directly compared. Yet, the principal relationships between sand content and flow dynamics were similar for both sets of experiments.

RESULTS

Experiment Set 1: Lock-exchange flume experiments adding 25% very fine sand or clay to high-density pure-clay flows


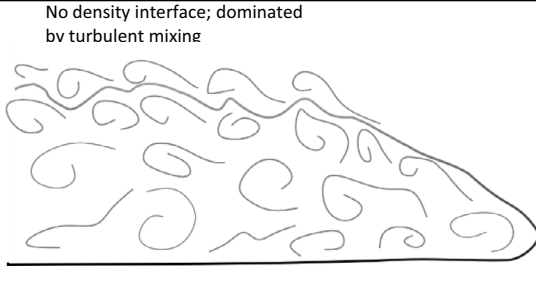

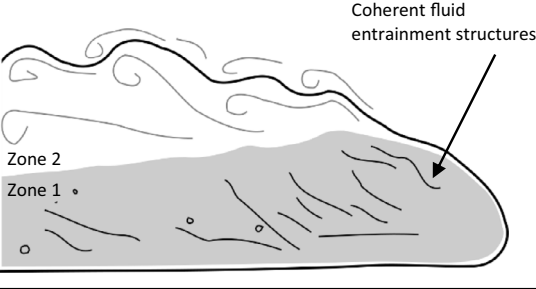
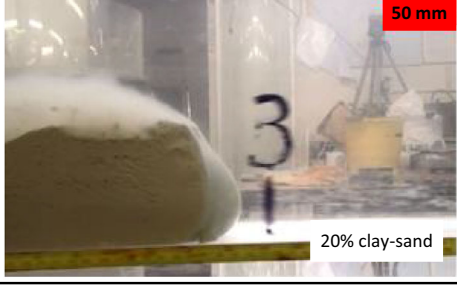
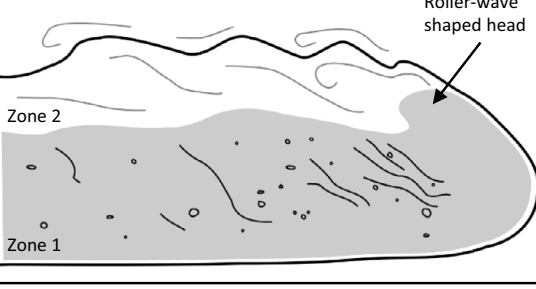

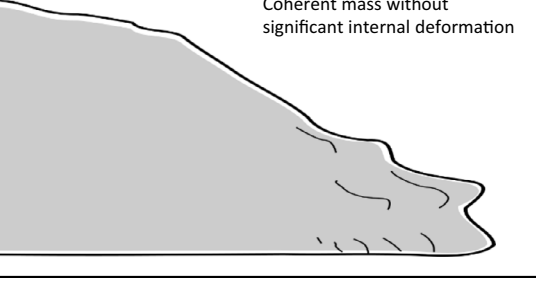
The flow behaviour, maximum head velocity and runout distances from the first set of

experiments on high-density cohesive SGFs are presented in Table 1 and Fig. 3, and each flow was visually classified into a flow type following Baker *et al.* (2017; Table 4). Below, the results are described separately for the two principal trios of experiments. First, the original 15% pure-clay flow is contrasted with the 18% clay-sand flow and the 18% control clay flow. Second, the original 16% pure-clay flow is compared to the 20% clay-sand and 20% control clay flows.

Adding 25% very fine sand or clay to the 15% pure-clay flow

Flow behaviour: The video recordings show that the 15% original pure-clay flow consisted of two zones: a dark lower zone 1 composed of a dense, quasi-laminar plug layer without visible mixing, and a lighter-coloured upper zone 2, where ambient water mixed into the flow and Kelvin-Helmholtz instabilities developed along the upper surface. The head of the 15% pure-clay flow had a pointed semi-elliptical shape with a prominent nose. Within zone 1, linear features of clear ambient water along the side-wall of the flume, defined as *coherent fluid entrainment structures* (Baker *et al.*, 2017), developed. The 18% clay-sand flow had the same two-part flow structure as the 15% pure-clay flow. However, the head of the 18% clay-sand flow was more rounded with a

Table 4. Summary of flow classifications, with example photographs and conceptual diagrams of heads of flows.

Flow classification	Photographic example	Interpretative drawing
Low-density turbidity current		
High-density turbidity current		
Mudflow/debris flow		
Slide		

lighter-coloured upper zone 2, and numerous coherent fluid entrainment structures were observed. Both the 15% pure-clay flow and the 18% clay-sand flow are classified as a high-density turbidity currents following Baker *et al.* (2017; Table 4).

The 18% control clay flow primarily comprised a dense laminar plug layer without coherent fluid entrainment structures, and a dilute

suspension cloud on the top of the flow. The flow had a blunt semi-circular head during the initial and final flow stages. The head of the flow lifted off the base of the flume and folded back on itself, attaining a roller-wave-like shape (Table 4). The 18% control clay flow is classified as a mud flow following Baker *et al.* (2017). Mud flows (containing grain sizes of $<63\ \mu\text{m}$) and debris flows (comprising all grain sizes) are

characterized by their strong to full turbulence suppression and limited mixing at the upper boundary (Baker *et al.*, 2017; Table 4).

Flow velocity and runout distance: The head velocity of all the experimental flows increased rapidly as the flows left the reservoir (Fig. 1A). The 15% pure-clay flow and 18% clay-sand flow accelerated to similar maximum head velocities of 0.35 m s^{-1} and 0.36 m s^{-1} , respectively, after which the head velocity of both flows stabilized, but with superimposed higher-frequency fluctuations. At distance from the lock gate, x , of 2.6 m the 18% clay-sand flow displayed a rapid decrease in velocity in the final flow stages to produce a runout distance of 3.52 m (Fig. 1A and C). In contrast, the head velocity of the 15% pure-clay flow reduced slightly from $x = 3.2 \text{ m}$ to $x = 4.4 \text{ m}$, before rapidly decelerating to zero resulting in a runout distance of 4.66 m. The 18% control clay flow accelerated to a maximum head velocity of 0.27 m s^{-1} . Once the maximum head velocity was reached, the flow then decelerated quickly to produce a runout distance of 1.42 m (Fig. 1A and C).

Adding 25% of very fine sand or clay to the 16% pure-clay flow

Flow behaviour: The 16% pure-clay flow had the same two-zone structure, pointed semi-elliptically shaped head, and coherent fluid entrainment structures in the dense lower layer as the 15% pure-clay flow. The 16% pure-clay flow is therefore also categorized as a high-density turbidity current (Baker *et al.*, 2017; Table 4). In contrast, the 20% clay-sand flow comprised a dense plug layer that lacked any noticeable internal turbulence or mixing with the ambient water, although a dilute suspension cloud developed at the front of the flow. The head of the 20% clay-sand flow curled back on itself before attaining a tall, rounded shape that was maintained until the final flow stages. Faint coherent fluid entrainment structures were observed in the lower zone from $x = 0.5$ to $x = 1.5 \text{ m}$. This behaviour of the 20% clay-sand flow describes a debris flow (Baker *et al.*, 2017; Table 4). The 20% control clay flow travelled out of the reservoir as a coherent mass for 0.22 m and did not mix with the ambient water. This flow lacked a clearly defined head and is classified as a slide following the definition of a high-density SGF that moves as a coherent

mass without significant internal deformation (Martinsen, 1994; Mohrig & Marr, 2003; Table 4).

Flow velocity and runout distance: The 16% pure-clay flow accelerated quickly once the lock gate was lifted and then maintained a reasonably constant head velocity until $x = 3.6 \text{ m}$. Thereafter, rapid flow deceleration produced a runout distance of 3.77 m (Fig. 1B and D). The 16% pure-clay flow had a maximum head velocity of 0.37 m s^{-1} , compared to 0.31 m s^{-1} for the 20% clay-sand flow. After the initial increase in head velocity upon leaving the reservoir, the 20% clay-sand flow gradually decelerated to $x = 1.5 \text{ m}$. The head velocity of the flow then rapidly decreased, resulting in a runout distance of 1.79 m. The 20% control clay flow displays a different velocity profile compared to those presented above; this flow reached a maximum head velocity of only 0.07 m s^{-1} before decelerating to a runout distance of 0.22 m (Fig. 1B and D).

Grain-size trends in the high-density mixed clay-sand deposits

The deposits of the mixed clay-sand flows were sampled to investigate vertical and horizontal changes in clay and sand percentage. These results are presented in Fig. 1E and 1F as percentage clay content. A reduction in percentage clay, and hence increase in percentage sand, represents a coarsening trend, whilst the opposite signifies a fining trend. Figure 1F demonstrates that the clay-sand deposit of the 20% flow lacked horizontal and vertical changes in clay percentage. In contrast, the clay-sand deposit of the 18% flow shows both horizontal and vertical variations in percentage clay (Fig. 1E). All sampled locations in the deposit demonstrate a fining-upward trend via a vertical increase in percentage clay. Along the deposit of the 18% clay-sand flow, the most proximal location, at $x = 0.20 \text{ m}$, had a slightly lower percentage clay in near-bed samples compared to the two more distal locations, which had similar grain-size profiles. For example, the deposit at $x = 0.20 \text{ m}$ 12.5 mm above the bed contained 77% clay compared to 78.5% clay at the same height above the bed at $x = 1.40 \text{ m}$ and 3.20 m (Fig. 1E). The base of the deposit of the 18% clay-sand flow therefore became modestly finer with distance from the lock gate until $x \approx 1.4 \text{ m}$; thereafter, the grain size was constant.

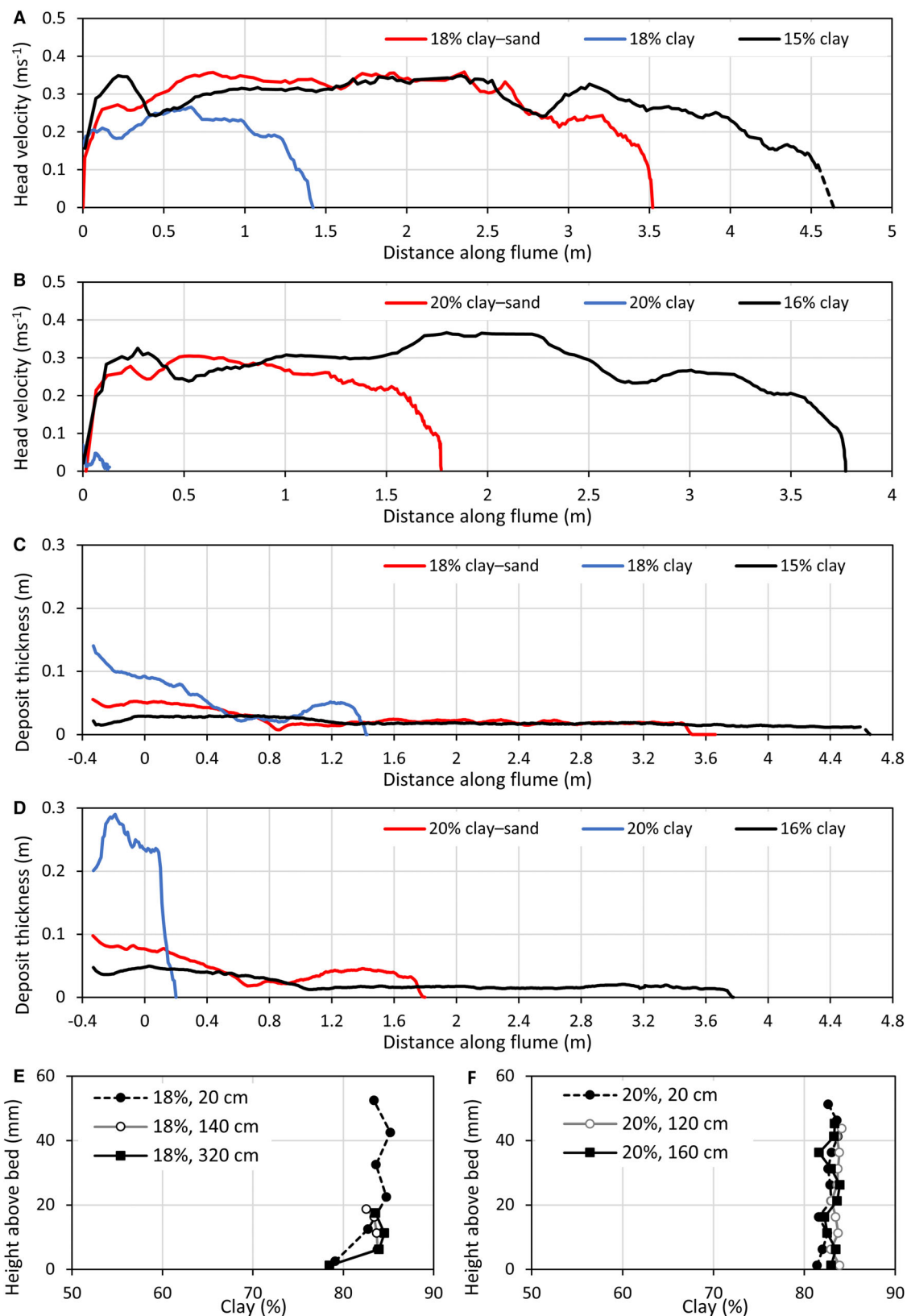


Fig. 1. (A) and (B) Head velocity, and (C) and (D) deposit thickness plots from Experiment Set 1, where the volume concentration of high-density flows is increased by 25% from the addition of very fine sand or clay. (E) Grain-size variations in the 18% clay-sand deposit. (F) Grain-size variations in the 20% clay-sand deposit.

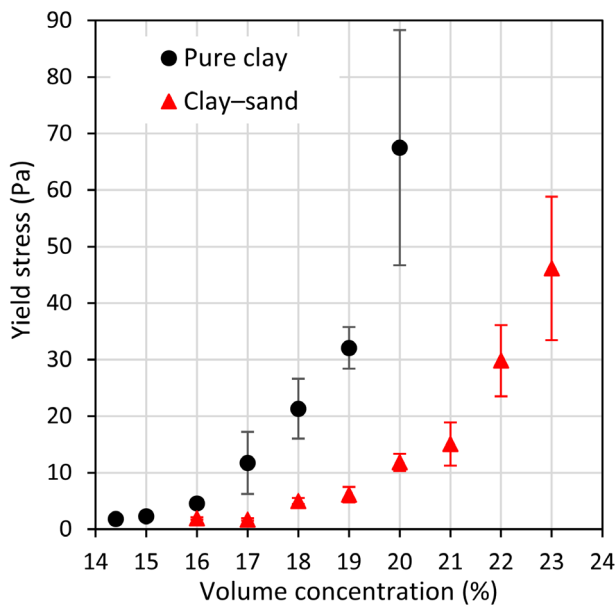


Fig. 2. Yield stress against concentration for pure-clay suspensions and mixed clay-sand suspensions at a ratio of 80:20 clay:sand, calculated from the runout distance of subaerial dam break experiments following the methods and theoretical equations of Balmforth *et al.* (2007) and Matson & Hogg (2007). The volume concentrations of the suspensions include the starting suspensions used in Experiment Set 1. Error bars are the 95% confidence intervals.

Starting suspension yield stress of the high-density cohesive sediment gravity flows

The yield stress of the starting suspensions used in the lock-exchange experiments for the high-density cohesive SGFs in Experiment Set 1 was calculated from the subaerial dam break experiments, following the methods of Balmforth *et al.* (2007) and Matson & Hogg (2007). These yield stress values demonstrate that increasing the volume concentration of the pure clay and mixed clay-sand suspensions increases the yield stress exponentially (Fig. 2). Figure 3A and 3D focus on the yield stress values of the suspensions used in the lock-exchange experiments and show that the yield stress of the pure clay suspensions increases after the addition of sand and clay. The yield stress of the 15% pure-clay suspension increased by a factor of 2.2, from 2.3 to 5.0 Pa, by adding sand to produce the 18% clay-sand suspension (Fig. 3A). These values compare to 21.3 Pa for the 18% control clay suspension. The 16% pure-clay suspension had a yield stress of 4.6 Pa. The addition of 25% sand increased the yield stress to 11.8 Pa for the 20%

clay-sand suspension, an increase of a factor of 2.5 (Fig. 3D). The 20% control clay suspension had a yield stress of 67.5 Pa in comparison. These results demonstrate that adding 25% sand to a high-concentration clay suspension causes a significant increase in yield stress, which was unexpected given that the sand particles were non-cohesive.

Experiment Set 2: Lock-exchange flume experiments adding 25% very fine sand to pure-clay flows across a large range of concentrations

Table 2 and Fig. 4 outline the changes in head velocity, flow behaviour and runout distance between the pure-clay flows and clay-sand flows, where the volume concentration was increased by adding 25% very fine sand, across a larger range of initial clay concentrations than in the first set of experiments.

Flow behaviour

The 10%, 12%, 13.5% and 14.4% pure-clay flows had pointed semi-elliptically shaped heads and were fully turbulent, i.e. without any internal density interface. These flows mixed readily with the ambient water to form Kelvin-Helmholtz instabilities, and they are classified as low-density turbidity currents (Baker *et al.*, 2017). Increasing the volume concentration of these flows by adding 25% sand to produce the 12.5%, 15%, 16.9% and 18% clay-sand flows generated flows with similar behaviour to their pure clay counterparts, dominated by strong turbulent mixing. The 12.5% to 18% clay-sand flows are therefore also categorized as low-density turbidity currents.

The 16% pure-clay flow comprised two zones: a lower quasi-laminar plug zone 1 covered by a lighter zone 2 that mixed with the ambient water. This flow behaviour is typical of high-density turbidity currents (Table 4). Adding sand to produce the 20% clay-sand flow made a flow that had the same two-zone structure as the 16% pure-clay flow, but with a thicker zone 1 and a more rounded head shape.

The 17% pure-clay flow also behaved as a high-density turbidity current with a dense lower layer and rounded head shape. In contrast, the 21.3% clay-sand flow comprised a dense plug flow that did not mix with the ambient water, although a weak suspension cloud developed as it travelled along the tank. The 21.3% clay-sand flow had a blunt semi-circular

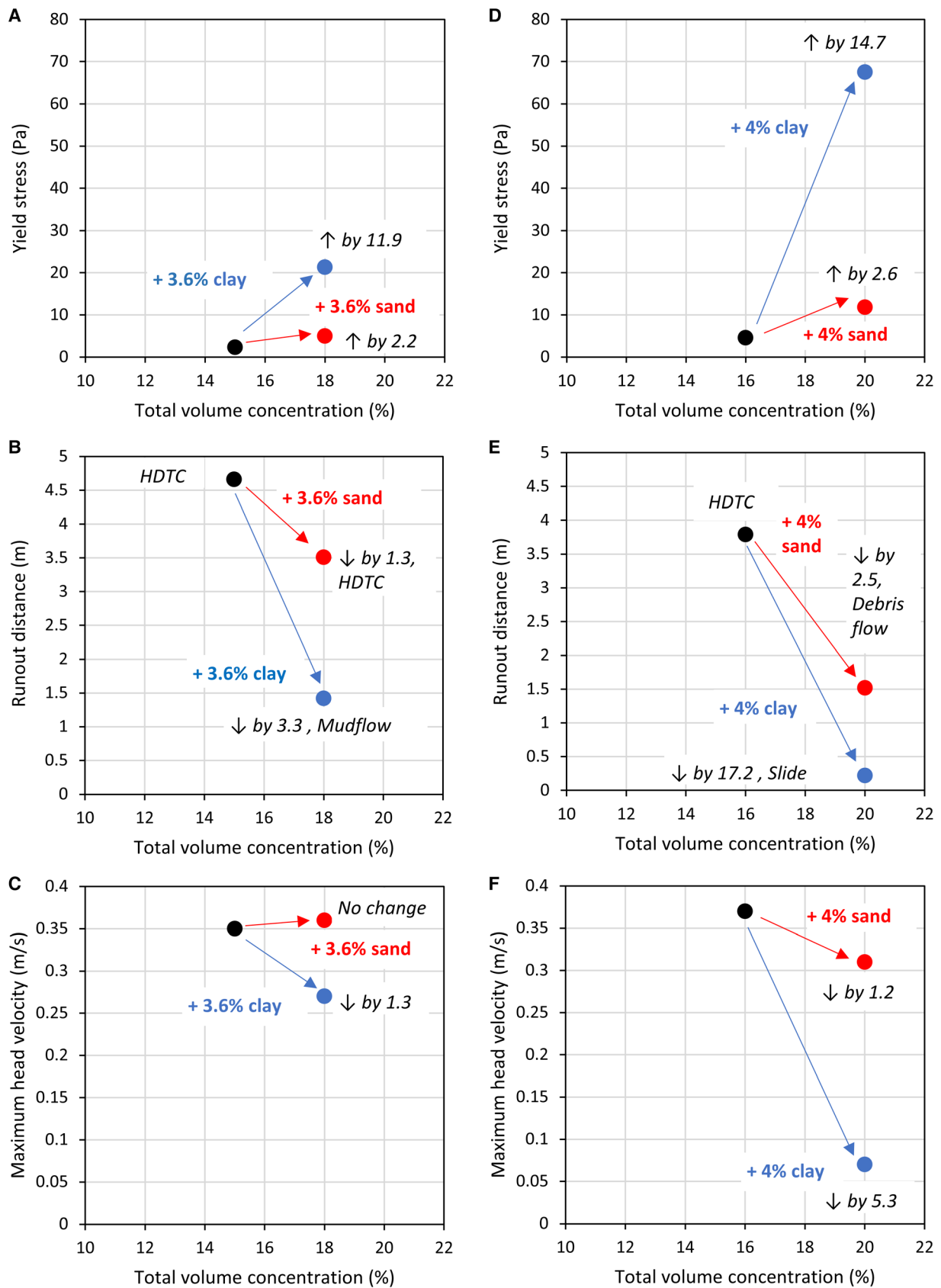


Fig. 3. Experiment Set 1 summary of changes in yield stress, runout distance and maximum head velocity for the (A) to (C) 15% pure-clay flow and (D) to (F) 16% pure-clay flow, when the volume concentration of the suspension is increased by 25% from the addition of very fine sand (red arrows and data points) or clay (blue arrows and data points). Factors of change in yield stress, runout distance and maximum head velocity from the original 15% or 16% pure-clay flows are shown in italics. In (B) and (E), the flow types are also displayed, HDTC, high-density turbidity current.

shaped head and is classified as a debris flow (Baker *et al.*, 2017).

Flow velocity and runout distance

All of the flows accelerated rapidly upon leaving the reservoir; thereafter, the head velocity decreased along the remainder of the flow path (Fig. 4). For the 10%, 12%, 13.5% and 14.4% pure-clay flows, increasing the volume concentration by adding 25% sand produced flows that accelerated to a greater maximum head velocity, and these greater head velocities remained along the length of the tank (Figs 4A to 4D and 5).

The 20% clay-sand flow was faster than the equivalent 16% pure-clay flow in the first 3 m along the tank, but the velocity difference was smaller than in the lower-concentration flows (Figs 4E and 5). The 20% clay-sand flow then decelerated rapidly to produce a runout distance of 3.68 m compared to 4.36 m for the 16% pure-clay flow (Fig. 4E).

The 21.3% clay-sand and 17% pure-clay flows had similar maximum head velocities and head velocity profiles at $x < 1.8$ m (Fig. 4F). The 21.3% clay-sand flow then decelerated quickly from $x = 2$ m to produce a runout distance of 2.39 m. The 17% pure-clay flow decelerated rapidly from $x \approx 3$ m and had a runout distance of 3.25 m.

PROCESS INTERPRETATIONS

The experimental results presented herein demonstrate that increasing the volume concentration by adding 25% sand or clay changes the flow behaviour, head velocity and runout distance of the high-density cohesive SGFs, as well as their suspension yield stress (Fig. 3). Adding very fine sand to the pure-clay flows first increased and then decreased the flow mobility, as the initial clay concentration was increased (Figs 4 and 5). The changes in flow behaviour and rheology of the high-density pure-clay flows in Experiment Set 1, along with the grain-size

trends in the mixed clay-sand deposits, are interpreted first. The effect of adding very fine sand across the larger range of cohesive SGF concentrations from Experiment Set 2 is discussed thereafter.

Experiment Set 1: Lock-exchange flume experiments adding 25% very fine sand or clay to high-density pure-clay flows

Adding 25% very fine sand or clay to the 15% pure-clay flow

Both the 15% pure-clay flow and 18% clay-sand flow were classified as high-density turbidity currents. Baker *et al.* (2017) interpreted high-density turbidity currents as flows in which the sediment is supported primarily by fluid viscosity from high clay concentrations. High-density turbidity currents can therefore be considered to have transitional, turbulence-modulated flow behaviour. The grain-size data for the deposit of the 18% clay-sand flow supports the high-density turbidity current classification. The modest upward and downflow fining of this deposit demonstrates that some sand was able to settle out of suspension as the flow travelled along the tank. This suspension settling is interpreted to occur in the lower transient-turbulent layer, i.e. zone 1, of the flow (Table 4). If the 18% clay-sand flow had behaved as a low-density turbidity current, the upward and downflow fining of sand would have been more pronounced. For flows characterized as laminar debris flows, no grading would be expected.

Despite both flows behaving as high-density turbidity currents, the flow behaviour changed when sand was added to the 15% pure-clay flow to produce the 18% clay-sand flow. The 18% clay-sand flow had a more rounded head than the 15% pure-clay flow and a lighter-coloured upper layer than the 15% pure-clay flow because of reduced mixing with the ambient water. These differences suggest that the 18% clay-sand flow had greater cohesive strength than the 15% pure-clay flow, because the flow was able to resist

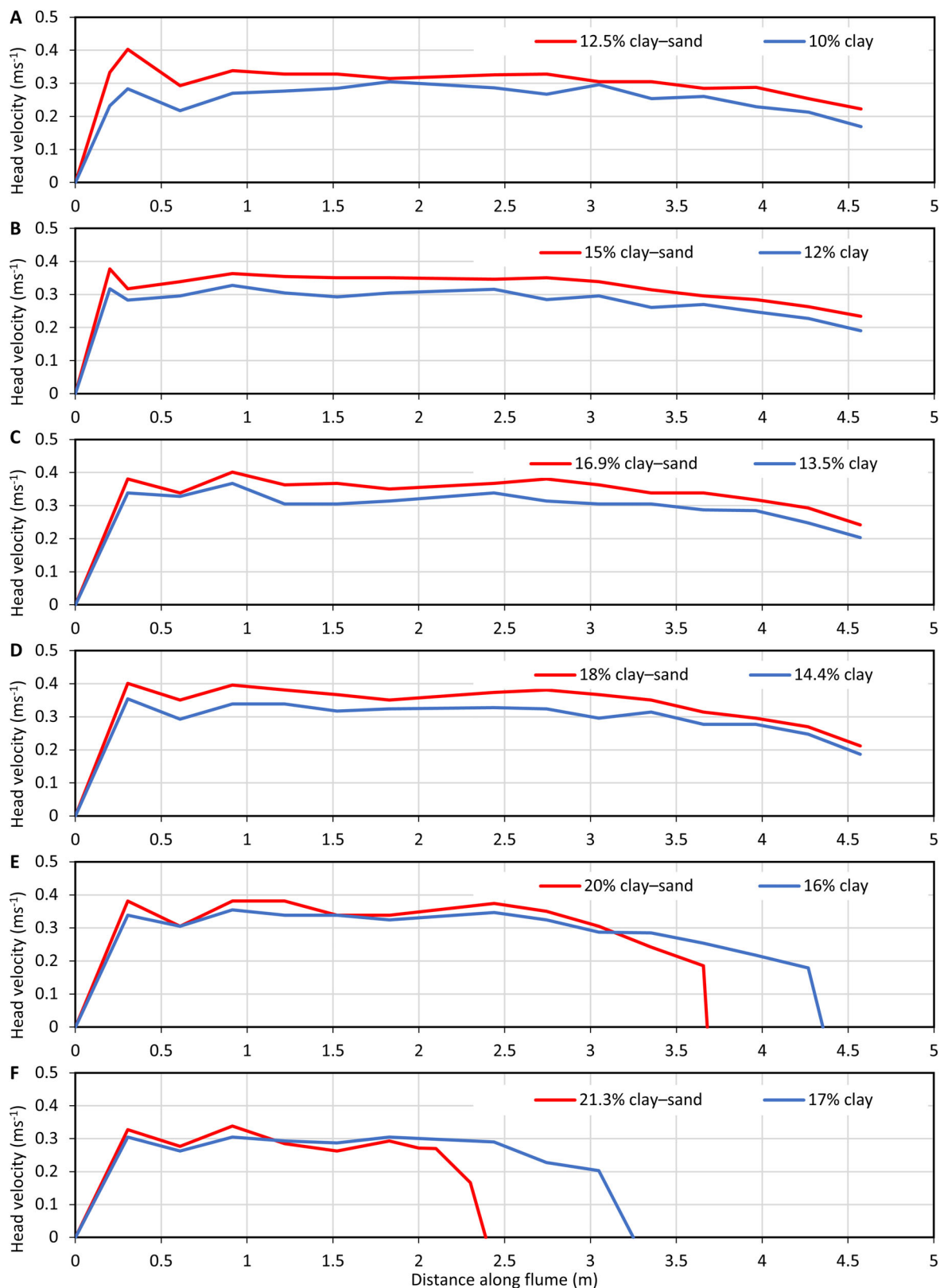


Fig. 4. Head velocity plots of pure-clay flows and clay-sand flows in Experiment Set 2, where the volume concentration of the pure-clay flows was increased by adding 25% very fine sand across a large range of initial clay concentrations.

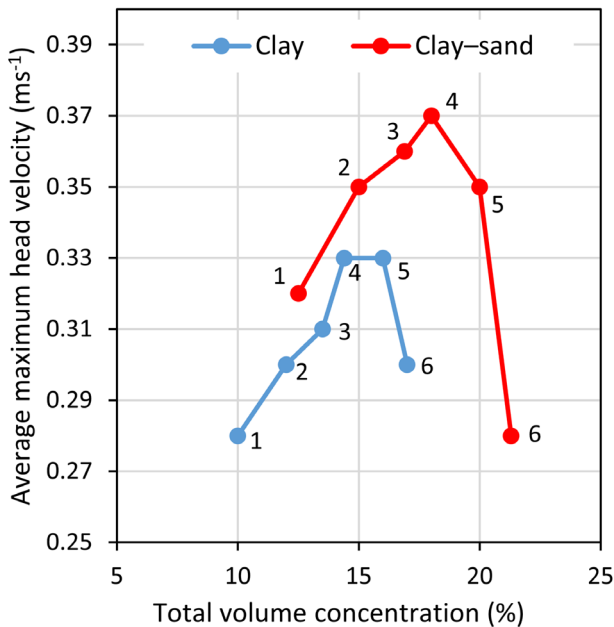


Fig. 5. Maximum head velocity plots of the clay and clay-sand flows, averaged from 1 m to 2 m along the length of the tank, from Experiment Set 2. Values represent the clay flow and its corresponding clay-sand flow where the volume concentration was increased by adding 25% very fine sand.

streamlining of the head by the ambient water and limit the shear-induced mixing in the upper zone 2 of the flow (Table 4).

The head velocity profiles demonstrate that the 18% clay-sand flow was less mobile than the 15% pure-clay flow (Figs 1A and 3C). Although both flows reached similar maximum head velocity values, the 18% clay-sand flow decelerated closer to the point of release than the 15% pure-clay flow. This resulted in a shorter runout distance for the 18% clay-sand flow (Figs 1A and 3B). It is inferred that, despite having a greater density difference with the ambient water, stronger cohesive forces in the 18% clay-sand flow were able to outcompete the turbulent forces closer to the point of release compared to the 15% pure-clay flow. The interpretations based on head shape and flow behaviour that the 18% clay-sand flow had greater cohesive strength than the 15% pure-clay flow are supported by the yield stress data, which show that the 18% clay-sand suspension had a higher yield stress than the 15% pure-clay suspension. The mechanisms that cause non-cohesive sand to increase the yield stress of clay suspensions are discussed below.

The 18% control clay flow had a lower head velocity and a shorter runout distance than both the 15% pure-clay flow and the 18% clay-sand flow (Figs 1A and 3B). The change in flow behaviour was also greater; the addition of 25% clay promoted flow transformation from a high-density turbidity current to a cohesive mud flow (Table 4). The 18% control clay suspension had a larger yield stress than both the 15% pure-clay and 18% clay-sand suspensions (Fig. 3A). The effects on the flow behaviour, flow mobility and suspension yield stress from the addition of 25% clay to the 15% pure-clay flow to produce the 18% control clay flow mirrors the results of Baker *et al.* (2017) in that, at these high clay concentrations, the clay particles are able to collide and form stronger clay flocs and gels, increasing the viscosity and shear strength of the flows at the expense of shear-induced turbulence.

Adding 25% very fine sand or clay to the 16% pure-clay flow

The reduction in flow mobility of the 18% clay-sand flow compared to the 15% pure-clay flow is mirrored when comparing the 20% clay-sand flow to the 16% pure-clay flow. The 16% pure-clay flow had a greater head velocity and was mobile for longer than the 20% clay-sand flow (Fig. 1B). This resulted in a shorter runout distance for the 20% clay-sand flow. The addition of 25% sand to the 16% pure-clay flow to produce the 20% clay-sand flow also enabled flow transformation. The 16% pure-clay flow was classified as a high-density turbidity current, whilst the 20% clay-sand flow behaved as a debris flow with a rounded, folded head and a dense plug that hardly mixed with the ambient water (Table 4). The absence of any changes in grain size throughout the deposit of the 20% clay-sand flow supports the debris-flow classification, as a laminar plug with strong to full turbulence suppression is required to produce non-graded deposits (Mulder & Alexander, 2001).

The mechanism responsible for these changes in flow behaviour and flow mobility between the 16% pure-clay flow and 20% clay-sand flow is interpreted to be the same as described above for the 15% pure-clay flow and 18% clay-sand flow. The addition of sand increased the cohesive strength of the flow, supported by the higher yield stress of the 20% clay-sand suspension compared to the 16% pure-clay suspension (Fig. 3D). This increase in cohesive strength outweighed the increased density difference

between the flow and the ambient fluid, thus reducing the flow mobility of the 20% clay–sand flow compared to the 16% pure-clay flow (Fig. 3E and F).

The 20% control clay flow slid out of the reservoir and had a runout distance of merely 0.22 m. This flow mobility was drastically lower than that of the 16% pure-clay flow and also considerably lower than that of the 20% clay–sand flow (Fig. 3E). This further supports the above interpretation that increasing the volume concentration by adding 25% clay to high-density cohesive SGFs increases the number and strength of cohesive bonds, leading to less mobile, turbulence-suppressed flow (Baker *et al.*, 2017).

Experiment Set 2: Lock-exchange flume experiments adding 25% very fine sand to pure-clay flows across a large range of concentrations

The second set of experiments demonstrates that the addition of very fine sand to cohesive SGFs can both increase and decrease the flow mobility.

The 10 to 14.4% pure-clay flows were classified as low-density turbidity currents. For these flows, the particles are supported by the upward component of fluid turbulence generated mainly at the boundaries of the flow (Middleton & Hampton, 1973). For the 10 to 14.4% pure-clay flows, the cohesive forces of the clay likely had a minimal influence on the flow dynamics, as the turbulence limited the formation of clay flocs and gels (*cf.* Baker *et al.*, 2017, table 3). Adding 25% sand to the 10 to 14.4% pure-clay flows increased the head velocity of these flows along the entire length of the tank (Fig. 4). This consistent increase in head velocity can be explained by the non-cohesive sand increasing the density difference between the flow and the ambient water, thus increasing the driving force, in the absence of sufficiently large cohesive forces.

In contrast, for the higher concentration 16% and 17% pure-clay flows, adding 25% very fine sand reduced the mobility and runout distance of these flows (Fig. 4). As already discussed for the first set of experiments, the addition of very fine sand to high-density clay flows appears to increase the cohesive strength of the flow. This greater cohesive strength outcompetes the increased density difference between the flow and the ambient fluid, thus reducing the flow mobility.

HOW DOES NON-COHESIVE SAND INCREASE THE YIELD STRESS OF HIGH-CONCENTRATION CLAY SUSPENSIONS?

The rheological data demonstrate that adding clay and adding sand to a dense clay suspension increases the suspension yield stress by a considerable amount (Fig. 3A and D), even though the sand is non-cohesive. These increases in yield stress and corresponding reductions in flow runout distance potentially have important consequences for predicting SGF mobility. It is therefore beneficial to discuss the physical processes responsible for the observed increases in yield stress. Increasing the concentration of clay in a suspension increases the number of clay particles and allows a greater number of electrostatic bonds to be formed between the clay particles, increasing the suspension yield stress (Baas & Best, 2002; Winterwerp & van Kesteren, 2004). The increase in yield stress with the addition of non-cohesive sand to the clay suspensions is in line with the limited amount of work published on the yield stress and apparent viscosity of mixed clay–sand suspensions containing a range of clay mineral types (Major & Pierson, 1992; Coussot & Piau, 1995; Ancey & Jorrot, 2001; Mahaut *et al.*, 2008). The processes responsible for increasing the yield stress by adding non-cohesive sand to a clay suspension are discussed below.

The behaviour of large non-cohesive particles, here sand, in a non-Newtonian suspension, here a clay suspension, is complex because of the variety of potential interactions between the particles (Mahaut *et al.*, 2008). To simplify the system, rheological studies consider the clay suspensions as a ‘yield stress fluid’ with non-cohesive particles embedded in the fluid (e.g. Ovarlez *et al.*, 2015). Following this approach, the term ‘particle’ refers exclusively to the non-cohesive sand particles from hereon. The potential interactions of the sand particles in the clay suspension can be divided into mechanical interactions and physicochemical interactions. Mechanical interactions encompass hydrodynamic particle–fluid interactions and physical particle–particle interactions, such as friction and collisions. Hydrodynamic particle–fluid interactions describe how the motion of a particle in a fluid induces a long-range flow field that is felt by other particles (Russel *et al.*, 1989). As particles react to these changes in the fluid’s local velocity, the forces required to maintain the flow are increased, and so is the fluid yield

stress (Yammine *et al.*, 2008). Physicochemical interaction defines particle-particle and particle-clay forces of attraction (Mahaut *et al.*, 2008).

Rheological studies have generally found that mechanical interactions are the main process by which the large non-cohesive particles increase the yield stress of non-Newtonian suspensions. Several lines of enquiry support this. Firstly, sand is inert without surface charge, as are the glass beads used in these experiments, which renders particle-particle and particle-clay forces of attraction unlikely. Secondly, Mahaut *et al.* (2008) designed and conducted experiments to evaluate the purely mechanical contribution of non-cohesive particles in yield stress fluids. Mahaut *et al.* (2008) found that for bentonite suspensions the addition of glass beads (of particle diameters 140 μm , 330 μm and 2000 μm) increased the measured yield stresses. Finally, theoretical rheological studies have demonstrated that mathematical models that include only the mechanical interactions correctly predict the observed changes in yield stress for a variety of particle and yield stress fluid types (e.g. Chateau *et al.*, 2008; Vu *et al.*, 2010; Ovarlez *et al.*, 2015).

Out of the mechanical interactions, hydrodynamic interactions are often considered to be the most important for the observed increase in yield stress of non-Newtonian suspensions containing particles (*cf.* Sengun & Probstein, 1989; Yammine *et al.*, 2008). In contrast, Ancey & Jorrot (2001) proposed 'depletion of clay particles' to explain the increase in yield stress they observed when glass beads or sand were added to a 25% kaolin clay suspension. Based on ideas from polymer science, Ancey & Jorrot (2001) suggested that in the close vicinity of large particles, the concentration of clay particles or flocs reduces because of spatial constraints. In the remaining space away from the large particles, the clay concentration thus increases slightly, and this increases the yield stress of the entire suspension (Russel *et al.*, 1989; Ancey & Jorrot, 2001). Ancey & Jorrot (2001) speculated that the depletion results either from surface repulsion forces between the kaolin particles and the coarse particles, or changes in the floc structure of the kaolin. For the clay-sand suspensions presented here, hydrodynamic particle-fluid interactions are hypothesized to be the most important mechanical interaction responsible for the observed increase in yield stress of the clay suspension from the addition of sand (*cf.* Sengun & Probstein, 1989; Yammine *et al.*, 2008;

Fig. 3). Physical particle-particle interactions, such as friction and collisions, are likely to be negligible, considering the low concentrations of sand (below 4.3%) in the present experiments. These low sand concentrations limit the opportunities for particles to collide and interact. The local depletion of clay particles near the large particles, as proposed by Ancey & Jorrot (2001), may occur. However, it seems unlikely that depletion results from repulsive forces between the inert glass beads and the clay particles, so yet unstudied changes in the clay floc or gel structure are deemed a more probable explanation.

DISCUSSION

Effect of adding sand to natural cohesive sediment gravity flows across a large range of flow behaviours

The present experiments have demonstrated that the addition of a small amount of non-cohesive very fine sand to cohesive SGFs can both increase and decrease the flow mobility, depending on how the inclusion of this sand changes the balance of turbulent and cohesive forces in the flow. These experiments have shown, for the first time, that the addition of very fine sand to high-density cohesive SGFs can increase the yield stress of clay suspensions and reduce the mobility of the flows. The mechanical interactions that are considered the main mechanism by which the sand increases the suspension yield stress are expected to occur also in natural suspensions (Mahaut *et al.*, 2008). Since natural cohesive SGFs are likely to contain at least some sand and silt, the effect of non-cohesive sediment on the cohesive properties of these SGFs needs to be considered. Below, a conceptual model for the effect of adding non-cohesive, very fine sand to cohesive SGFs is suggested for the full range of initial flow conditions.

For weakly cohesive flows that behave as low-density turbidity currents in the natural environment, the low clay concentration renders the clay minerals unable to collide and flocculate, and thus turbulent forces dominate these flows. As demonstrated by the experiments, the addition of a small amount of very fine sand to low-density turbidity currents, for example, by the erosion of sandy substrates under natural conditions, increases the density difference driving

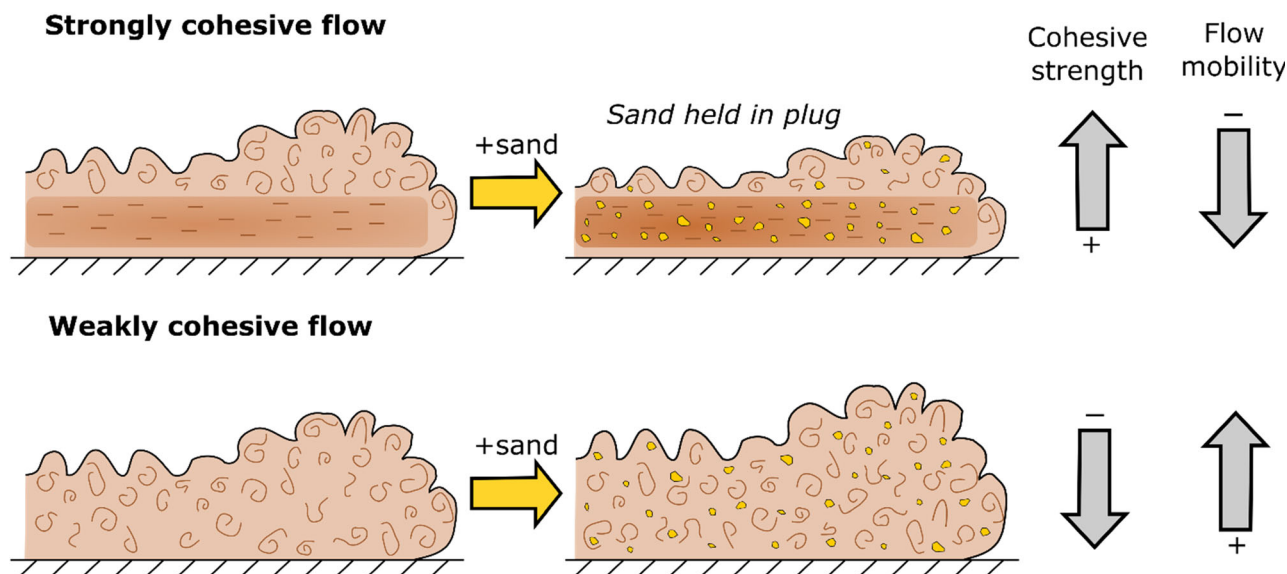


Fig. 6. Conceptual diagram of how the addition of a small volume of sand may change the flow mobility of cohesive sediment gravity flows. For high-density, strongly cohesive sediment gravity flows (SGFs) dominated by transitional or laminar flow behaviour, the addition of a small amount of non-cohesive sediment is expected to increase the cohesive strength of the plug layer, instigating a reduction in flow mobility. If sand is added to weakly cohesive flows dominated by turbulent forces, adding sand will enhance the density difference, promote turbulent mixing, and increase the flow mobility.

the flow, and this should increase the flow velocity and further promote turbulent mixing (Fig. 6). Adding greater amounts of very fine sand will further increase the excess density and flow velocity until the flow is saturated with sand and the particles can no longer be supported. Grain-to-grain interactions between the sand particles then dampen turbulent forces and limit flow mobility, and the flow likely undergoes 'frictional freezing' and *en masse* deposition (Mulder & Alexander, 2001). Baker *et al.* (2017) showed, for silt particles, that frictional freezing happens at ultra-high concentrations of *ca* 50% by volume.

For high-density, strongly cohesive SGFs dominated by transitional or laminar flow behaviour, such as high-density turbidity currents and mud flows, the addition of a small amount of non-cohesive, very fine sand is expected to increase the cohesive strength of the dense, laminar plug layer. The increase in cohesive strength of the plug layer results in a reduction in flow mobility, despite the increase in density excess, as observed in the present experiments (Fig. 6). The increased cohesive strength of the flow could result in flow transformation to more cohesive flow behaviour, for example from high-density turbidity current to debris flow, or from

debris flow to slide. This is supported by the present laboratory experiments; the addition of 25% very fine sand to the 16% pure-clay flow in the first set of experiments enabled flow transformation from a high-density turbidity current to a debris flow (Table 4). For the highest-density cohesive flows, such as slides, it is suggested that adding any amount of very fine sand will reduce the flow mobility by promoting bulk settling.

The threshold at which the addition of very fine sand may increase or decrease the flow mobility of a cohesive SGF is challenging to predict, and dependent on the volume of sand added and the initial cohesive strength of the flow. The initial cohesive strength of the flow is a function of multiple parameters, including clay concentration, clay mineral type, flow velocity, ratio of cohesive to non-cohesive sediment and extent of biological cohesion (Marr *et al.*, 2001; Ilstad *et al.*, 2004; Baas *et al.*, 2009; Baker *et al.*, 2017; Hermidas *et al.*, 2018; Craig *et al.*, 2020). For example, previous work has demonstrated that flows containing weakly cohesive kaolinite clay and strongly cohesive bentonite clay show the same changes in suspension yield stress and flow mobility as clay concentration is increased, but the threshold

concentration above which clay modulates the flow behaviour is lower for bentonite flows (Baas *et al.*, 2016b; Baker *et al.*, 2017). It is therefore expected that a higher initial clay concentration within kaolinite-rich flows is needed to produce a similar cohesive strength of bentonite-rich flows. However, an increase in yield stress from the addition of non-cohesive sand to clay suspensions has been demonstrated to be irrespective of clay mineral type (Major & Pierson, 1992; Coussot & Piau, 1995; Ancey & Jorrot, 2001; Mahaut *et al.*, 2008). The cohesive strength of a flow is also expected to vary in space and time as cohesive bonds break and reform under the changing flow stresses. In the laboratory experiments presented here, initial clay concentration can be used as an indicator for cohesive strength of the flow. For the second set experiments, the initial clay concentration threshold where the addition of a small amount of very fine sand started to reduce, rather than increase, flow mobility fell between 14.4% and 16% clay. It is expected that for full-scale natural flows, the clay concentration where the addition of a small amount of very fine sand reduces flow mobility will be higher, as natural flows are often faster and more turbulent (Talling *et al.*, 2013), and therefore more likely to break the bonds between clay particles. As such, higher clay concentrations will be needed to produce flows that have a dense, laminar plug layer, where the addition of very fine sand to this layer is expected to increase the suspension yield stress. Focusing on the flow behaviour, rather than flow concentration, may be a more practical indicator for how the addition of a small amount of very fine sand may change natural flows. The authors propose that, for flows that contain a dense plug layer, i.e. high-density turbidity currents, the addition of a small amount of very fine sand is likely to reduce flow mobility. For flows without a plug layer that are dominated by turbulent mixing, the addition of very fine sand is likely to promote further turbulent mixing and enhance flow mobility.

Further work is needed to determine how changing the volume of added sand controls the mobility of high-density cohesive SGFs. The design of such experiments should also investigate the physical mechanisms for changes in yield stress from the addition of sand to high-density cohesive SGFs and establish the boundaries of sand concentration that hinder or promote the flow mobility. More experiments are also needed to investigate the effect of the size

of non-cohesive particles. This work should focus on the role of turbulent and cohesive forces in keeping particles of different size in suspension and the development of density stratification, which may control the minimum clay concentration at which non-cohesive particles start to cause a decrease in flow mobility.

Role of sand in flow transformation across submarine fans

Whilst travelling on submarine fans, SGFs can exhibit flow type transformation as a result of changing boundary conditions (Talling *et al.*, 2012). In the proximal part of submarine fans, i.e. canyons and channels, SGFs are often highly mobile and erosive because of steep slope gradients, lateral confinement and high sediment concentrations (e.g. Babonneau *et al.*, 2002; Paull *et al.*, 2018). Clay-rich flows in this part of submarine fans are likely to have a high flow velocity that promotes strong turbulent mixing and impedes the formation of cohesive bonds between clay minerals. If these cohesive SGFs erode non-cohesive sand from the substrate, the density difference with the ambient water is enhanced and these flows should accelerate, as demonstrated by the present experiments. If these cohesive flows erode cohesive clay from the bed, the opportunity for clay minerals to collide, flocculate and gel increases. Above a critical amount of eroded clay, the flows start to decelerate, as enhanced cohesive forces suppress the turbulent forces, limiting the flow mobility and promoting transformation to flows dominated by cohesive forces (Baas & Best, 2002; Baas *et al.*, 2009; Sumner *et al.*, 2009; Baker *et al.*, 2017). However, submarine canyons and channels are typically dominated by coarse-grained, non-cohesive deposits, such as massive sands (Babonneau *et al.*, 2010; Bernhardt *et al.*, 2011), rendering the erosion of clay-rich deposits less likely in this part of submarine fans.

Sediment gravity flows that travel across the distal region of submarine fans, between the lobe and distal fringe, have been found to transform from turbulent to laminar as the cohesive forces become increasingly dominant over the turbulent forces (Kane *et al.*, 2017). This results in the formation of transitional flow deposits and hybrid event beds (Barker *et al.*, 2008; Houghton *et al.*, 2009; Kane & Pontén, 2012). The mechanisms for causing flow transformation are the entrainment of mud from the substrate

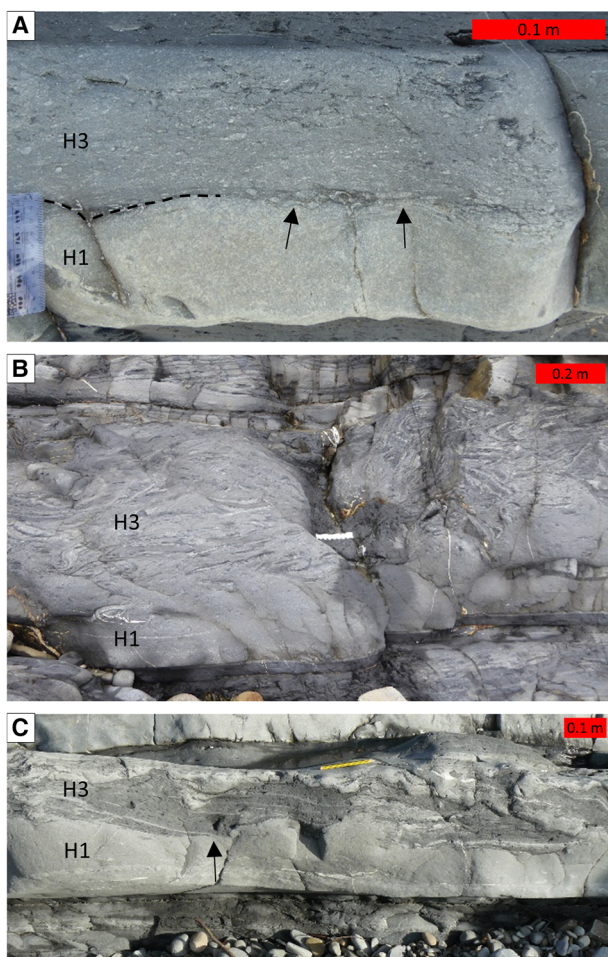


Fig. 7. Examples of hybrid event beds in the Aberystwyth Grits Group where sand from the H1 division is incorporated in the mud-rich H3 division. (A) Sandstone clasts (arrows) at the base of a H3 division, eroded from the bed below. (B) Gradual boundary between the H1 and H3 divisions, interpreted as sand incorporated from an earlier deposited turbidite in the mixed clay-sand debris flow of a hybrid event. (C) Uneven top of H1 division, suggesting erosion by a debris flow that formed the H3 division above; the arrow shows how an elongated sand clast in H3 links to the H1 division below.

into the flows (Hodgson, 2009) and the deceleration of the flows, allowing the cohesive forces in the flow to dampen turbulence (Kane *et al.*, 2017). The results from the present experiments suggest that the presence of sand in high-density cohesive SGFs can also increase the yield stress of the flow and promote flow transformation.

The addition of sand to clay-rich SGFs may occur via scouring of sand-rich SGF deposits.

Although cohesive flows with damped turbulence are not as erosional as fully turbulent flows, laboratory experiments have demonstrated that decelerating sand-silt-clay transitional flows can produce scour features because of enhanced near-bed turbulence (Baas *et al.*, 2011, 2016a). An important field example relevant to the present study is the erosion of sand from the H1 division in a developing hybrid event bed by a debris flow that forms the H3 division (Haughton *et al.*, 2009). This addition of sand to the debris flow may reduce its mobility by increasing the cohesive strength, and thus promote deposition of the H3 division on top of the H1 division. In the Aberystwyth Grits Group and Borth Mudstone Formation (Wales, UK), the H3 divisions of hybrid event beds have been observed to contain sand eroded from the H1 division below (Baker & Baas, 2020; Fig. 7). In the Gottero turbidite system (north-west Italy), Fonnesu *et al.* (2017) observed that rafts in the H3 division of their Type 1 and Type 2 hybrid event beds contained thin-bedded sandstone-mudstone heterolithics, which could often be matched to the substrate beneath the event bed (their figs 6 and 15C). These substrate rafts were observed to disintegrate and be partly incorporated into the flow down-dip (Fonnesu *et al.*, 2017). Both sets of field observations provide evidence for the addition of sand to clay-rich SGFs, which, through ensuing flow deceleration, may help to explain the common association of sandy turbidites and mixed clay-sand debris-flow deposits in hybrid event beds.

CONCLUSIONS

The lock-exchange experiments demonstrate that the addition of a small amount of non-cohesive, very fine sand to cohesive sediment gravity flows can both increase and decrease the flow mobility, depending on the initial balance of turbulent and cohesive forces in the flow. For flows dominated by turbulent forces, such as low-density turbidity currents, adding a small amount of very fine sand to the laboratory flows increases the excess density driving the flows, resulting in faster flow. For high-density cohesive sediment gravity flows, i.e. high-density turbidity currents and mud flows, adding the very fine sand produces mixed clay-sand flows with stronger cohesive behaviour, lower head velocities and shorter runout distances than the

original clay flows. The yield stress measurements demonstrate that adding non-cohesive, very fine sand increases the yield stress of the high-density starting suspensions. Comparison with previous work suggests that mechanical interactions between the sand particles and the clay suspension are the main process by which the yield stress is increased. The enhanced cohesive strength of the mixed clay-sand flows attenuates the turbulent forces, and thus reduces the flow mobility, despite the greater density difference between the flow and ambient water, and the non-cohesive nature of the sand particles.

In the natural environment, the effect of adding non-cohesive sediment on the cohesive strength of cohesive sediment gravity flows needs to be considered, whilst also accounting for the effect of enhanced excess density. This study suggests that non-cohesive sediment only increases the yield stress and reduces the flow mobility of strongly cohesive sediment gravity flows, where the sand can be supported within the cohesive matrix. For weakly cohesive sediment gravity flows, the sand is likely to promote turbulence mixing in the flow and increase the flow mobility.

The present experiments have demonstrated that non-cohesive sand increases the cohesive strength, via the yield stress, of high-concentration clay suspensions. This implies that the cohesive strength of natural cohesive sediment gravity flows containing clay, sand and silt should not be considered only in terms of the clay concentration. The change in flow behaviour and rheology from the addition of very fine sand may have important implications for flow transformation, particularly in the distal region of mud-rich submarine fans.

ACKNOWLEDGEMENTS

We are very grateful to Rhian Tait and Abigail Smyth for their help in the laboratory, funded by the Bangor University Undergraduate Internship Scheme. Equinor funded MLB's PhD studentship that enabled this research to be undertaken, using the flume facility kindly built by Bangor University technician Rob Evans. The Associate Editor Kyle Straub, Elisabeth Steel and one anonymous reviewer are thanked for their thorough and in-depth comments which greatly improved the manuscript.

DATA AVAILABILITY STATEMENT

The data that support the findings of this study are available from the corresponding author upon reasonable request.

REFERENCES

- Ancey, C. and Jorrot, H. (2001) Yield stress for particle suspensions within a clay dispersion. *J. Rheol.*, **45**, 297–319.
- Baas, J.H. and Best, J. (2002) Turbulence modulation in clay-rich sediment-laden flows and some implications for sediment deposition. *J. Sed. Res.*, **72**, 336–340.
- Baas, J.H., Best, J.L. and Peakall, J. (2011) Depositional processes, bedform development and hybrid bed formation in rapidly decelerated cohesive (mud-sand) sediment flows. *Sedimentology*, **58**, 1953–1987.
- Baas, J.H., Best, J.L. and Peakall, J. (2016a) Predicting bedforms and primary current stratification in cohesive mixtures of mud and sand. *J. Geol. Soc. London*, **173**, 12–45.
- Baas, J.H., Best, J.L. and Peakall, J. (2016b) Comparing the transitional behavior of kaolinite and bentonite suspension flows. *Earth Surf. Proc. Land.*, **41**, 1911–1921.
- Baas, J.H., Best, J.L., Peakall, J. and Wang, M. (2009) A phase diagram for turbulent, transitional, and laminar clay suspension flows. *J. Sed. Res.*, **79**, 162–183.
- Babonneau, N., Savoye, B., Cremer, M. and Bez, M. (2010) Sedimentary architecture in meanders of a submarine channel: detailed study of the present Congo turbidite channel (ZAIANGO project). *J. Sed. Res.*, **80**, 852–866.
- Babonneau, N., Savoye, B., Cremer, M. and Klein, B. (2002) Morphology and architecture of the present canyon and channel system of the Zaire deep-sea fan. *Mar. Petrol. Geol.*, **19**, 445–467.
- Baker, M.L. and Baas, J.H. (2020) Mixed sand-mud bedforms produced by transient turbulent flows in the fringe of submarine fans: indicators of flow transformation. *Sedimentology*, **67**, 2645–2671.
- Baker, M.L., Baas, J.H., Malarkey, J., Jacinto, R.S., Craig, M.J., Kane, I.A. and Barker, S. (2017) The effect of clay type on the properties of cohesive sediment gravity flows and their deposits. *J. Sed. Res.*, **87**, 1176–1195.
- Balmforth, N.J., Craster, R.V., Perona, P., Rust, A.C. and Sassi, R. (2007) Viscoplastic dam breaks and the Bostwick consistometer. *J. Non-Newton Fluid*, **142**, 63–78.
- Barker, S.P., Houghton, P.D.W., McCaffrey, W.D., Archer, S.G. and Hakes, B. (2008) Development of rheological heterogeneity in clay-rich high-density turbidity currents: Aptian Britannia sandstone member, U.K., Continental Shelf. *J. Sed. Res.*, **78**, 45–68.
- Bernhardt, A., Jobe, Z.R. and Lowe, D.R. (2011) Stratigraphic evolution of a submarine channel-lobe complex system in a narrow fairway within the Magallanes foreland basin, Cerro Toro formation, southern Chile. *Mar. Petrol. Geol.*, **28**, 785–806.
- Chateau, X., Ovarlez, G. and Trung, K.L. (2008) Homogenization approach to the behavior of suspensions of noncolloidal particles in yield stress fluids. *J. Rheol.*, **52**, 489–506.
- Coussot, P. and Piau, J.M. (1995) The effects of an addition of force-free particles on the rheological properties of fine suspensions. *Can. Geotech. J.*, **32**, 263–270.

- Craig, M.J., Baas, J.H., Amos, K.J., Strachan, L.J., Manning, A.J., Paterson, D.M., Hope, J.A., Nodder, S.D. and Baker, M.L. (2020) Biomediation of submarine sediment gravity flow dynamics. *Geology*, **48**, 72–76.
- Fonnesu, M., Felletti, F., Haughton, P.D.W., Patacci, M. and McCaffrey, W.D. (2017) Hybrid event bed character and distribution linked to turbidite system sub-environments: the north Apennine Gottero sandstone (north-West Italy). *Sedimentology*, **65**, 151–190.
- Haughton, P.D.W., Davis, C., McCaffrey, W. and Barker, S.P. (2009) Hybrid sediment gravity flow deposits - classification, origin and significance. *Mar. Petrol. Geol.*, **26**, 1900–1918.
- Hermidas, N., Eggenhuisen, J.T., Jacinto, R.S., Luthi, S.M., Toth, F. and Pohl, F. (2018) A classification of clay-rich subaqueous density flow structures. *J. Geophys. Res.: Earth Surf.*, **123**, 945–966.
- Hodgson, D.M. (2009) Distribution and origin of hybrid beds in sand-rich submarine fans of the Tanqua depocentre, Karoo Basin, South Africa. *Mar. Petrol. Geol.*, **26**, 1940–1956.
- Ilstad, T., Elverhøi, A., Issler, D. and Marr, J.G. (2004) Subaqueous debris flow behaviour and its dependence on the sand/clay ratio: a laboratory study using particle tracking. *Mar. Geol.*, **213**, 415–438.
- Kane, I.A. and Pontén, A.S.M. (2012) Submarine transitional flow deposits in the Paleogene Gulf of Mexico. *Geology*, **40**, 1119–1122.
- Kane, I.A., Pontén, A.S.M., Vangdal, B., Eggenhuisen, J.T., Hodgson, D.M. and Spychala, Y.T. (2017) The stratigraphic record and processes of turbidity current transformation across deep-marine lobes. *Sedimentology*, **64**, 1236–1273.
- Kneller, B.C. and Buckee, C. (2000) The structure and fluid mechanics of turbidity currents: a review of some recent studies and their geological implications. *Sedimentology*, **47**, 62–94.
- Lowe, D.R. and Guy, M. (2000) Slurry-flow deposits in the Britannia formation (lower cretaceous), North Sea: a new perspective on the turbidity current and debris flow problem. *Sedimentology*, **47**, 31–70.
- Mahaut, F., Chateau, X., Coussot, P. and Ovarlez, G. (2008) Yield stress and elastic modulus of suspensions of noncolloidal particles in yield stress fluids. *J. Rheol.*, **52**, 287–313.
- Major, J.J. and Pierson, T.C. (1992) Debris flow rheology: experimental analysis of fine-grained slurries. *Water Resour. Res.*, **28**, 841–857.
- Marr, J.G., Harff, P.A., Shanmugam, G. and Parker, G. (2001) Experiments on subaqueous sandy gravity flows: the role of clay and water content in flow dynamics and depositional structures. *Geol. Soc. Am. Bull.*, **113**, 1377–1386.
- Martinsen, O. (1994) Mass movements. In: *The Geological Deformation of Sediments* (Ed. Maltman, A.), pp. 127–165. Chapman and Hall, London.
- Matson, G.P. and Hogg, A.J. (2007) Two-dimensional dam break flows of Herschel-Bulkley fluids: the approach to the arrested state. *J. Non-Newton fluid*, **142**, 79–94.
- Middleton, G.V. (1966) Experiments on density and turbidity currents. I. Motion of the head. *Can. J. Earth Sci.*, **3**, 523–546.
- Middleton, G.V. and Hampton, M.A. (1973) Sediment gravity flows: mechanics of flow and deposition. In: *Turbidity and Deep Water Sedimentation* (Eds Middleton, G.V. and Bouma, A.H.), pp. 1–38. SEPM Pacific Section, Short Course Lecture Notes.
- Mohrig, D. and Marr, J.G. (2003) Constraining the efficiency of turbidity current generation from submarine debris flows and slides using laboratory experiments. *Mar. Petrol. Geol.*, **20**, 883–899.
- Mulder, T. and Alexander, J. (2001) The physical character of subaqueous sedimentary density flow and their deposits. *Sedimentology*, **48**, 269–299.
- Ovarlez, G., Mahaut, F., Deboeuf, S., Lenoir, N., Hormozi, S. and Chateau, X. (2015) Flows of suspensions of particles in yield stress fluids. *J. Rheol.*, **59**, 1449–1486.
- Parker, G., Fukushima, Y. and Pantin, H.M. (1986) Self-accelerating turbidity currents. *J. Fluid Mech.*, **171**, 145–181.
- Paull, C.K., Talling, P.J., Maier, K.L., Parsons, D., Xu, J., Caress, D.W., Gwiazda, R., Lundsten, E.M., Anderson, K., Barry, J.P. and Chaffey, M. (2018) Powerful turbidity currents driven by dense basal layers. *Nature Comms.*, **9**, 1–9.
- Russel, W., Saville, D. and Schowalter, W. (1989) *Colloidal Dispersions*, Cambridge Monographs on Mechanics. Cambridge University Press, Cambridge, 525 pp.
- Sengun, M.Z. and Probstein, R.F. (1989) Bimodal model of slurry viscosity with applications to coal slurries. Part 1. Theory and experiment. *Rheol. Acta.*, **28**, 382–393.
- Sumner, E.J., Talling, P.J. and Amy, L.A. (2009) Deposits of flows transitional between turbidity current and debris flow. *Geology*, **37**, 991–994.
- Talling, P.J. (2013) Hybrid submarine flows comprising turbidity current and cohesive debris flow: deposits, theoretical and experimental analyses, and generalized models. *Geosphere*, **9**, 460–488.
- Talling, P.J. (2014) On the triggers, resulting flow types and frequencies of subaqueous sediment density flows in different settings. *Mar. Geol.*, **352**, 155–182.
- Talling, P.J., Masson, D.G., Sumner, E.J. and Malgesini, G. (2012) Subaqueous sediment density flows: depositional processes and deposit types. *Sedimentology*, **59**, 1937–2003.
- Talling, P.J., Paull, C.K. and Piper, D.J.W. (2013) How are subaqueous sediment density flows triggered, what is their internal structure and how does it evolve? Direct observations from monitoring of active flows. *Earth Sci. Rev.*, **125**, 244–287.
- Vu, T.S., Ovarlez, G. and Chateau, X. (2010) Macroscopic behavior of bidisperse suspensions of noncolloidal particles in yield stress fluids. *J. Rheol.*, **54**, 815–833.
- Wang, Z. and Plate, E.C.H.J. (1996) A preliminary study on the turbulence structure of flows of non-Newtonian fluid. *J. Hydraul. Res.*, **34**, 345–361.
- Wells, M. and Dorrell, R. (2021) Turbulent processes within turbidity currents. *Annu. Rev. Fluid Mech.*, **53**, 59–83.
- Winterwerp, J.C. and van Kesteren, W.G.M. (2004) *Introduction to the Physics of Cohesive Sediment in the Marine Environment*. Elsevier, Oxford, 559 pp.
- Yammine, J., Chaouche, M., Guerinet, M., Moranville, M. and Roussel, N. (2008) From ordinary rheology concrete to self compacting concrete: a transition between frictional and hydrodynamic interactions. *Cem. Concr. Res.*, **38**, 890–896.

Manuscript received 4 February 2022; revision accepted 20 December 2022